JOURNAL OF MATERIALS SCIENCE **40** (2005) 5721–5726

Formation and growth studies of the $(Bi,Pb)_2Sr_2Ca_2Cu_3O_{10}$ phase in Ag sheathed tapes

X. P. CHEN
Applied Superconductivity Research Center,Tsinghua University, Beijing, 100084, People's Republic of China

J.-C. GRIVEL
Materials Research Department,Risø National Laboratory, DK-4000 Roskilde, Denmark
E-mail: jean-claude.grivel@risoe.dk

M. Y. LI, T. M. QU, Z. HAN, Q. LIU
Applied Superconductivity Research Center,Tsinghua University, Beijing, 100084, People's Republic of China

N. H. ANDERSEN
Materials Research Department,Risø National Laboratory, DK-4000 Roskilde, Denmark

Published online: 25 August 2005

The formation and the thickness growth of the $(Bi,Pb)_2Sr_2Ca_2Cu_3O_{10}$ phase in Ag-sheathed tapes have been investigated by scanning electron microscopy on samples sintered at 840°C in a flow of 8.5% O_2 (rest N_2) and quenched in air after sintering for 1 to 50 h. The thickness of the $(Bi,Pb)_2Sr_2Ca_2Cu_3O_{10}$ grains was measured statistically after different sintering times. The experimental results show that the average thickness of these grains increases during the entire sintering period, while the average thickness growth rate decreases exponentially with sintering time. The volume fractions of the various phases present during the heat treatment were also measured from micrographs. Detailed studies of the microstructure and phase formation kinetics support the view that the formation of the $(Bi,Pb)_2Sr_2Ca_2Cu_3O_{10}$ phase proceeds via a nucleation and growth process. Based on the present observations, a model describing the microstructure evolution is presented.

1. Introduction

The manufacture of $(Bi,Pb)_2Sr_2Ca_2Cu_3O_{10}$/Ag (Bi-2223/Ag) tapes with well oriented microstructure and capable of carrying large currents at the boiling temperature of nitrogen (77 K) is of great technical and economical interest for the development of low-loss power devices. A sound understanding of the Bi-2223 phase formation mechanism would help in optimising the standard industrial "powder-in-tube" (PIT) manufacturing process. In the PIT process, a mixture of precursor powders that do not contain the Bi-2223 phase is packed into a Ag tube. This composite is mechanically deformed by drawing and rolling in order to form a tape with typical dimensions of 3 mm width, 200 μm thickness and up to several hundred meters length. This green tape is then heat treated at high temperature in order to convert the precursor powders into the Bi-2223 phase. In order to maximise the current transport capability of the tape, a dense and well-oriented microstructure is necessary. In practice, non-superconducting phases are always present at the end of the process and the degree of preferential orientation of the Bi-2223 grains is far from optimum. As a consequence, a large number of studies have been devoted to describing the evolution of phase and microstructure development both in bulk and tapes samples during heat-treatments.

Numerous reports based on scanning electron microscopy/energy dispersive spectroscopy (SEM/EDS), transmission electron microscopy (TEM) and X-ray diffraction studies on quenched samples have been published [1–21]. Additionally, high-temperature *in-situ* measurements by means of synchrotron X-ray radiation [22, 23] and neutron scattering [24] were reported. However, open questions still remain as to the details of this formation mechanism and the associated microstructure development inside the Ag-sheathed Bi-2223 tape. The high complexity of this mechanism requires further studies devoted to a more detailed understanding.

Two main models have been presented for describing the formation of Bi-2223 from the precursor powders. The first model, nucleation and growth, considers that the Bi-2223 grains nucleate directly from a

0022-2461
DOI: 10.1007/s10853-005-0945-8

liquid phase, preferentially on $Bi_2Sr_2CaCu_2O_8$ (Bi-2212) grains present in large amount in the precursor powders [1, 6, 13]. The second model, intercalation, assumes that Bi-2212 crystals convert directly into Bi-2223 crystals via the insertion of CuO_2/Ca bilayers into the CuO_2/Ca/CuO_2 blocks of the Bi-2212 structure [25, 26]. The arguments in favour of the first of these models being much stronger, the nucleation and growth model is now commonly accepted.

In spite of this, not all details of the formation mechanism of the Bi-2223 phase are clear yet. Among the well-established facts, a liquid, which is known to result from a reaction between Bi-2212 and Pb-rich secondary phases, is formed during the high-temperature sintering [1, 6, 12, 13, 27]. In order to study the kinetics of the Bi-2223 phase formation via this liquid phase, the Avrami relation for isothermal transformations [28] has been used by various authors who conducted experiments using mostly X-ray diffraction techniques [21, 29–36]. Their main results were related to the 2-dimensional growth of the Bi-2223 platelets. However, the growth kinetics of the platelets along the *c*-axis direction has not been studied in much details, in particular the relationship between the thickness of the Bi-2223, the sintering time and the microstructure evolution of the tapes is not known. Garnier *et al.* [21] reported a kinetics study based on X-ray diffraction in bulk samples quenched after relatively long sintering times in order to map the late stages of phase transformation, where thickness growth plays a dominant role. In this report we present a systematic study of the Bi-2223 platelet growth during the sintering of Bi-2223/Ag tapes, using samples quenched after various equilibration times. The thickness of the Bi-2223 grains has been measured from polished cross-sections by means of scanning electron microscopy and the Bi-2223 phase formation kinetics has been performed using the Avrami relation. The mechanism of Bi-2223 formation and microstructure evolution of the ceramic core of the tapes is discussed on the basis of the present observations.

2. Experimental

A monofilament tape has been produced by the powder-in-tube method. The nominal composition of the precursor powder was $Bi_{1.8}Pb_{0.33}Sr_{1.87}Ca_{2.0}Cu_{3.0}O_{10+\delta}$. The initial phase assemblage of these precursor powders was Bi-2212, Ca_2PbO_4, $Bi_{0.5}Pb_3Sr_{2.5}Ca_2CuO_{12+\delta}$ and $(Ca,Sr)_{14}Cu_{24}O_{41}$. Samples of the tape used in the experiment were typically 3 mm wide, 0.2 mm thick and 50 mm long. The samples were sintered at 840°C in an 8.5% O_2 (rest N_2) atmosphere and air-quenched after sintering for 1, 2, 3, 5, 10, 20 or 50 h. This temperature has been chosen based on previous work on similar tapes [37].

Cross-section images of these samples were obtained from a Leo-1530 scanning electron microscope (SEM). The Bi-2223, Bi-2212, alkaline-earth cuprates and areas assumed to have resulted from the fast solidification of a liquid phase present at high temperature can be distinguished clearly in the backscattered electron imaging mode. At least two typical regions of each sample were selected for the measurements. The average thickness of Bi-2223 plate-shaped crystallites (i.e. measured along the *c*-axis of the Bi-2223 structure) was determined by measuring the thickness of about 100 Bi-2223 platelets in each sample. To obtain qualitative information about the kinetics of the Bi-2223 phase formation from the precursor powders, the fractional area of the Bi-2223, Bi-2212, secondary phases and the quenched liquid phase were determined from the polished tape cross-sections by SEM. The relative error on the measurements is estimated between 5 and 10%. The fractional area data were assumed to be equivalent to the volume fraction of the phases.

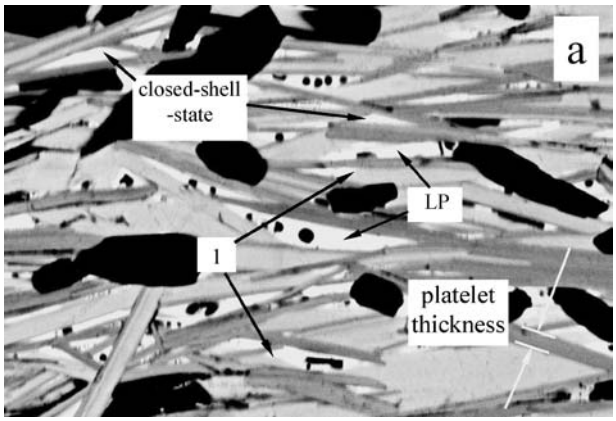

Figure 1 Backscattered SEM image of a polished cross-section of a sample sintered for 5 h at 840°C. 1: Coexistence of Bi-2212 and liquid, LP: quenched-in liquid phase, "closed-shell-state": liquid phase area surrounded by Bi-2223 grains. Width of picture: 30 μm.

3. Results and discussion

Fig. 1 shows a typical SEM backscattered electron micrograph of a sample quenched after 5 h sintering. The white regions are assumed to be the liquid phase formed at high temperature and quenched-in during the fast cooling process. The dark grey and light grey areas are the Bi-2223 and Bi-2212 phases respectively, while the black particles are alkaline-earth cuprates and CuO. In a previous study, the composition of the quenched liquid was analysed using a statistical method [37]. The EDS results showed that this material is rich in Bi and Pb, in agreement with earlier reports [6, 38]. In the precursor powders, Bi-2212 is the only phase containing a non-negligible amount of Bi. The presence of significant amounts of Bi in the liquid phase implies that the Bi-2212 phase melts to form it, or at least a part of it, during the sintering process of the tape. This is a strong argument in favour of the nucleation and growth mechanism [1, 6, 13]. It can be clearly observed that in many areas, Bi-2223 platelets are situated at the interface between Bi-2212 and the liquid phase, indicating that Bi-2223 easily nucleates and grows onto the *ab*-plane of Bi-2212 grains. The large aspect ratio of the Bi-2223 grains already at this early stage of reaction-sintering, shows that the phase grows much faster within its *ab*-plane than along its *c*-axis. The preferential nucleation of Bi-2223 at the interface between the Bi-2212 and liquid phases suggests that the similarity of both structures results in a low interfacial energy between Bi-2212 and Bi-2223.

As shown on the surface of bulk samples [13] and further suggested by the areas marked with "1" in

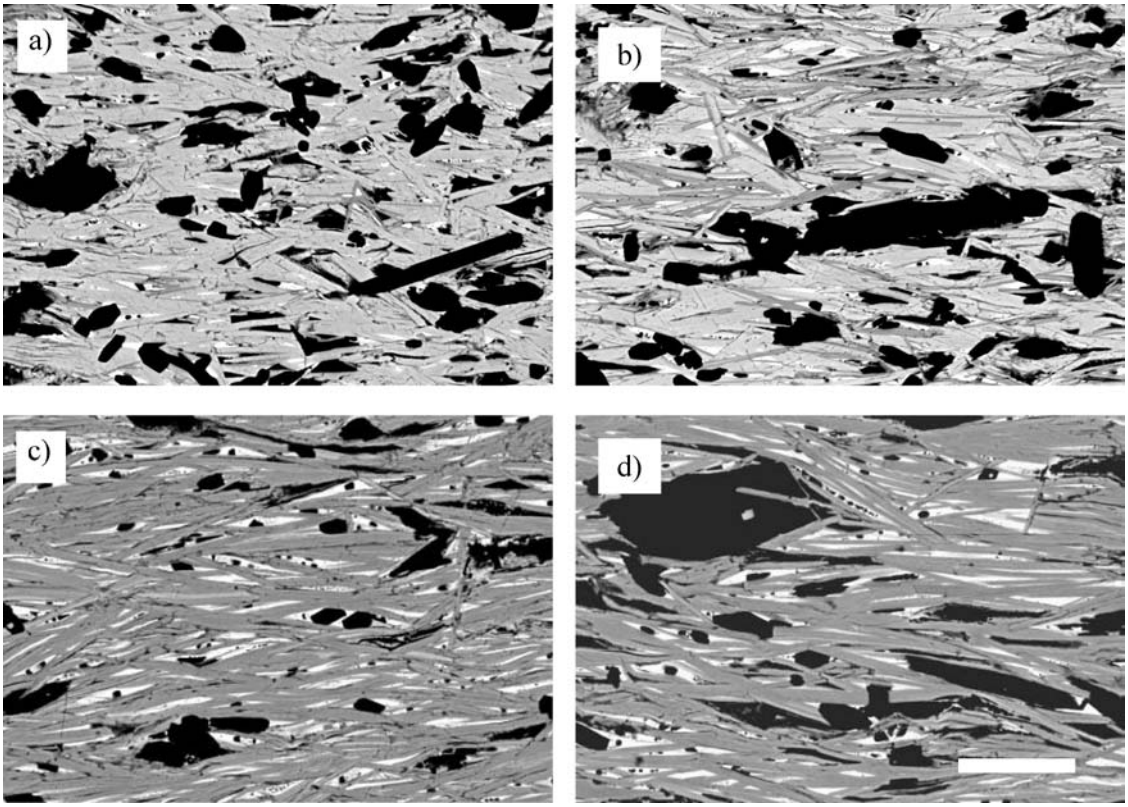

Figure 2 Backscattered SEM image of polished cross-sections of samples quenched after 1 h (a), 3 h (b), 10 h (c) and 50 h (d) sintering at 840°C. Length of white scale-label: 6 μm.

Fig. 1, the Bi-2212 phase melts progressively. Since the Bi-2212 phase does not completely disappear before the beginning of the Bi-2223 phase formation, the average texture of the two phases is similar, in accordance with previous observations [39–41], which showed that the texture of the new Bi-2223 grains inherit the average texture of the initial Bi-2212 grains. In fact, the similarity of the structure of both compounds makes Bi-2212 an ideal substrate for the growth of Bi-2223.

In most cases, the liquid regions are rapidly completely surrounded by Bi-2223 platelets. We will call this situation a "closed-shell-state" (see Fig. 1). Polished cross sections only represent a 2-dimensional cut in a 3-dimensional structure. We can therefore not ensure that all liquid areas defined as above actually are completely enclosed by Bi-2223. However, the large aspect ratio of the Bi-2223 platelets suggests that the "closed-shell-state" geometry extends significantly along the thickness of the sample, reducing the contact area between liquid and non-Bi-2223 phases to a negligible value.

The cross-section SEM back-scattering micrographs of samples quenched after sintering for different times (1, 3, 10 and 50 h) are shown in Fig. 2a–d. It is clearly seen that some Bi-2223 grains are already present in the sample after 1 h. With the sintering time increasing from 1 h to 3 h, both the amount of Bi-2223 grains and the volume fraction of this phase increase significantly. The thickness of the Bi-2223 platelets also increases. When the sintering time is longer than 10 h, there is almost no Bi-2212 phase left. It is also found that the "closed-shell-state" configuration seldom appears prior to 3 h sintering, where most liquid phase pockets are

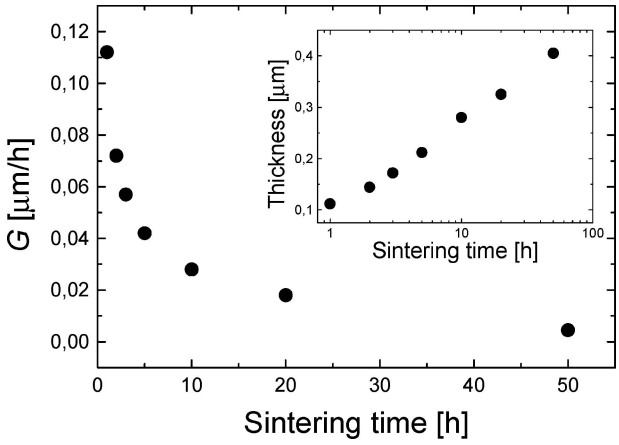

Figure 3 Thickness growth rate of Bi-2223 platelets G versus sintering time. Inset: average thickness of Bi-2223 platelets versus sintering time.

in contact with Bi-2212 at least on one side, whereas nearly all the liquid areas are surrounded by Bi-2223 platelets after 10 h or more.

The evolution of the average Bi-2223 platelet thickness as a function of time is shown in the inset of Fig. 3. The measurements show that the average thickness d increases during the entire sintering period. In particular, during the initial 10 h of sintering, d increases more rapidly. An average growth rate G defined as $G = \delta d / \delta t$ is presented in Fig. 3 versus sintering time. Apparently, the average growth rate of the Bi-2223 platelets perpendicular to the Cu-O planes decreases exponentially with sintering time. However, a quantitative analysis of the time dependence of G would probably be meaningless and will therefore not be attempted here. In fact, resulting from an averaging over many unrelated

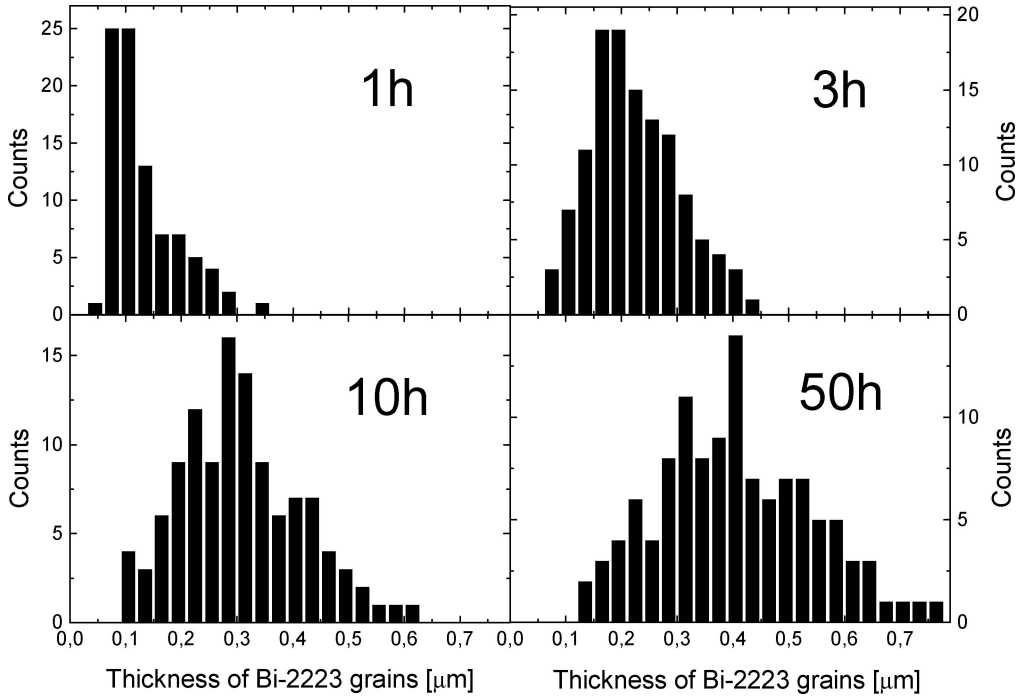

Figure 4 Histograms showing the distribution of Bi-2223 platelet thickness after sintering for 1, 3, 10 and 50 h.

grains, G only represents an *apparent* average growth rate. Several spurious effects can contribute to its observed decrease:

(a) Due to geometrical constraints, the Bi-2223 platelets cannot grow beyond a certain thickness defined by the local microstructure and amounting to 0.15 to 0.75 μm. Therefore, some grains that already stopped growing along their c-axis before quenching are inevitably included in the statistics. The proportion of such grains becomes higher as the sintering time increases, thus influencing the G values, mostly for $t_{\text{sintering}} \geq 10$ h.

(b) The inhomogeneities in the ceramic microstructure result in large variations of the local Bi-2223 growth conditions. For example, the liquid locked in "closed-shell-state" areas does not receive any more feed material from Bi-2212 and secondary phases. The growth rate, being in principle dependent on the concentration of solute in the liquid, will progressively decrease, until liquid pockets eventually remain that cannot contribute to Bi-2223 formation any more. Such effects, again, mainly take place at $t_{\text{sintering}} \geq 10$ h, i.e., when the "closed-shell-state" becomes a predominant feature of the overall microstructure.

(c) For the strong initial decrease of G, the following effect may be at play. After one hour sintering, only the thickening of platelets nucleated during the very first stage of reaction (i.e. $t_{\text{sintering}} \leq 1$ h) is taken into account in the statistics. Most of these platelets will grow further. But if new ones nucleate between 1 and 2 h sintering, some of these new grains will inevitably be included in the statistics for 2 h sintering. Since these newly nucleated particles got less time for growing than those nucleated earlier, they will result in a lowering of the average thickness and therefore induce an apparent decrease of the average growth rate G. This spurious effect will only disappear when the Bi-2223 nucleation rate becomes negligible. From our measurements, we can estimate that this is the case after 3 to 5 h, when we cannot see grains thinner than 0.1 μm any more (Fig. 4).

In order to extract qualitative information about the kinetics of the reactions leading to the formation of the Bi-2223 phase, the area fraction of Bi-2223, Bi-2212, liquid phase and secondary phases were determined from the SEM micrographs. These two-dimensional data were assumed to be equivalent to the volume fraction. The $V(t)$ evolution of the first three phases are plotted in Fig. 5 versus sintering time. Two time ranges can be defined. In the first range (0–10 h), the volume fraction of both the Bi-2223 and liquid phase increase sharply, while the volume fraction of Bi-2212 decreases rapidly. In the second range (10–50 h), the variations are much more gradual. After 50 h, the Bi-2212 phase disappeared almost completely.

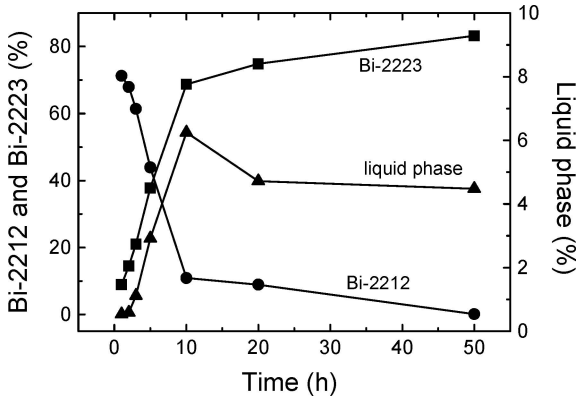

Figure 5 Volume fraction of Bi-2212, Bi-2223 and quenched-in liquid phases versus sintering time.

The evolution of the liquid phase volume during these two stages shows an interesting feature. During the first stage, its volume fraction increases with the sintering time and reaches a maximum after 10 h sintering. The volume fraction of Bi-2212, which is the main source of liquid phase, decreases rapidly during the first stage of phase formation and reaches 10% at 10 h. Beyond this point, the decomposition of the remaining Bi-2212 phase is much slower. The formation rate of the liquid phase is expected to follow a similar trend. However, the actual volume fraction of liquid phase is smaller than that of the Bi-2212 phase decomposed after a given sintering time. This is attributed to the rapid consumption of the liquid phase during the fast formation of Bi-2223 during the first reaction stages. After 10 h sintering, the formation rate of the liquid phase can no more compete with its consumption rate and the global liquid phase volume decreases.

In several reports, quantitative information about the kinetics of Bi-2223 phase formation has been extracted from the time evolution of the Bi-2223 volume fraction [24, 30–35]. In general, the Avrami-Erofe'ev model was found to be the best suited to fit the experimental data. In this model, the volume fraction of Bi-2223, $V(t)$, is expressed as followed:

$$V(t) = 1 - \exp(-kt^n)$$

where k is the rate constant, t is the equilibration time at the reaction temperature and n is an exponent dependent on the nature and characteristics of the transformation [28]. Fig. 6 shows the ln(-ln(1 − V)) versus ln$t$ behaviour. It exhibits two main distinct linear regions. For 2 h $\leq t \leq$ 10 h, n takes the value 1.3 (n_1 in Fig. 6). For prolonged sintering ($t >$ 10 h), n is equal to 0.3 (n_2 in Fig. 6). Such values are similar to those previously reported in kinetics analyses [21, 29, 30, 35]. However, the quantitative significance of those numbers is somewhat doubtful [42]. In fact, the Bi-2223 phase formation mechanism is a multi-step process and the standard kinetics models were developed for single-step reactions, as is the case for the Avrami model. Furthermore, a liquid phase is involved in the reaction chain, while most models have been derived for solid-state transformations.

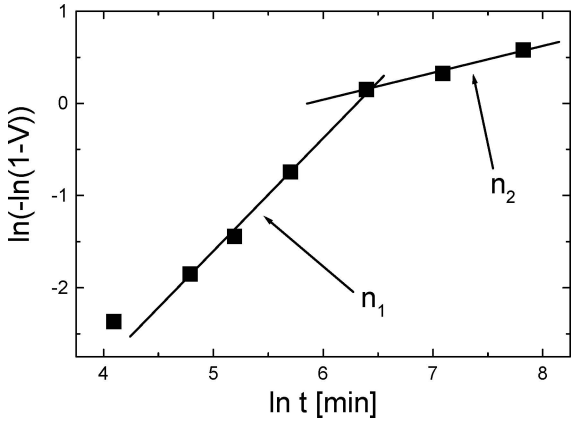

Figure 6 Avrami plot for the volume fraction (V) of the Bi-2223 phase.

In principle, a n value close to 1.5 indicates the growth of particles that nucleated only at the start of the transformation [43]. In the present case, "start of the transformation" is equivalent to the time interval preceding the linear segment yielding the n_1 exponent value, i.e. $t \leq$ 2 h sintering. This is in good qualitative agreement with our observations of thickness variation, where it was found that no new Bi-2223 grains appeared for $t \geq 3 - 5$ h. On the other hand, the $n_2 =$ 0.3 value obtained during the latest stage is not far from 0.5 that would reflect thickening of platelets after impingement of their edges [43]. Such a change of growth kinetics is also qualitatively consistent with the SEM observations (Figs 1 and 2), where it is found that the "closed-shell-state" is a predominating microstructural feature at $t \geq$ 10 h. In other words, the edges of most Bi-2223 platelets have impinged onto other grains so that growth within the *ab*-plane is no longer possible, while the *c*-axis growth is still not finished [21, 35].

It thus appears that, although the n-exponents do not strictly correspond to the values expected from the model calculations, the overall shape of the Bi-2223 phase volume evolution can be qualitatively explained on the basis of microstructural observations. A quantitative analysis of the phase formation kinetics however requires that the different steps of the Bi-2223 formation process are separated and studied individually.

4. Summary

Our microstructural observations provide further evidence for the nucleation and growth model, i.e. progressive melting of the Bi-2212 grains resulting in the formation of liquid pockets of restricted volume, followed by dissolution of secondary phases into the liquid. Bi-2223 precipitates preferentially at the liquid/Bi-2212 interface. The reaction then goes deeper into the liquid through precipitation and *c*-axis growth of Bi-2223.

The average growth rate of the Bi-2223 platelets perpendicular to the Cu-O plane decreases with time. However, this decrease may only be apparent and governed by the fact that it was not possible to follow the thickness evolution of one and the same grain during the sintering process.

Under the present conditions (840°C in 8.5% O_2), a liquid phase forms in Bi-2223/Ag tapes. Its volume fraction increases with sintering time and reaches a maximum at 10 h. During this initial stage, the growth of the Bi-2223 crystallites can proceed both along the *c*-axis and within the *ab*-plane of the structure, as long as the edges of the growing platelets have not impinged on neighbouring grains. After 10 h sintering however, all liquid regions are covered by the Bi-2223 platelets, the growth of which then occurs along the *c*-axis direction only.

References

1. T. HATANO, K. AOTA, S. IKEDA, K. NAKAMURA and K. OGAWA, *Jpn. J. Appl. Phys.* **27** (1988) L2055.
2. H. NOBUMASA, K. SHIMIZU, Y. KITANO and T. KAWAI, *ibid.* **27** (1988) L846.

3. A. OOTA, K. OHBA, A. ISHIDA, A. KIRIHIGASHI, K. IWASAKI and H. KUWAJIMA, *ibid.* **28** (1989) L1171.
4. Y. T. HUANG, C. Y. SHEI, W. N. WANG, C. K. CHIANG and W. H. LEE, *Physica C* **169** (1990) 76.
5. S. HORIUCHI, K. SHODA, X. J. WU, H. NOZAKI and M. TSUTSUMI, *ibid.* **168** (1990) 205.
6. P. E. D. MORGAN, R. M. HOUSLEY, J. R. PORTER and J. J. RATTO, *ibid.* **176** (1991) 279.
7. A. K. SARKAR, Y. J. TANG, X. W. CAO, J. C. HO and G. KOZLOWSKI, *Mat. Res. Bull.* **27** (1992) 1.
8. P. E. D. MORGAN, J. D. PICHÉ and R. M. HOUSLEY, *Physica C* **191** (1992) 179.
9. J.-C. GRIVEL, A. JEREMIE, B. HENSEL and R. FLÜKIGER, *Supercond. Sci. Technol.* **6** (1993) 725.
10. Y. E. HIGH, Y. FENG, Y. S. SUNG, E. E. HELLSTROM and D. C. LARBALESTIER, *Physica C* **220** (1994) 81.
11. S. C. KWON, H. G. LEE, B. T. AHN and S. W. NAM, *Supercond. Sci. Technol.* **7** (1995) 552.
12. Q. Y. HU, H. K. LIU and S. X. DOU, *Physica C* **250** (1995) 7.
13. J.-C. GRIVEL and R. FLÜKIGER, *Supercond. Sci. Technol.* **9** (1996) 555.
14. S. STASSEN, A. RULMONT, M. AUSLOOS and R. CLOOTS, *Physica C* **270** (1996) 135.
15. J. L. MACMANUS-DRISCOLL and Z. YI, *Supercond. Sci. Technol.* **10** (1997) 970.
16. K. FISCHER, T. FAHR, A. HÜTTEN, U. SCHLÄFER, M. SCHUBERT, C. RODIG and H.-P. TRINKS, *ibid.* **11** (1998) 995.
17. D. P. GRINDATTO, J.-C. GRIVEL, G. GRASSO, H.-U. NISSEN and R. FLÜKIGER, *Physica C* **298** (1998) 41.
18. J.-C. GRIVEL and R. FLÜKIGER, *Supercond. Sci. Technol.* **11** (1998) 288.
19. J.-C. GRIVEL, D. P. GRINDATTO, G. GRASSO and R. FLÜKIGER, *ibid.* **11** (1998) 110.
20. V. A. MARONI, M. TEPLITSKY and M. W. RUPICH, *Physica C* **313** (1999) 169.
21. V. GARNIER, I. MONOT-LAFFEZ and G. DESGARDIN, *ibid.* **349** (2001) 103.
22. Y. L. WANG, W. BIAN, Y. ZHU, Z. X. CAI, D. O. WELCH, R. L. SABATINI, M. SUENAGA and T. R. THURSTON, *Appl. Phys. Lett.* **69** (1996) 580.
23. T. FRELLO, H. F. POULSEN, L. G. ANDERSEN, N. H. ANDERSEN, M. D. BENTZON and J. SCHMIDBERGER, *Supercond, Sci. Technol.* **12** (1999) 293.
24. E. GIANNINI, E. BELLINGERI, R. PASSERINI and R. FLÜKIGER, *Physica C* **315** (1999) 185.
25. Z. X. CAI, Y. ZHU and D. O. WELCH, *Phys. Rev. B* **52** (1995) 13035.
26. W. BIAN, Y. ZHU, Y. L. WANG and M. SUENAGA, *Physica C* **248** (1995) 119.
27. A. ONO, *Jpn. J. Appl. Phys.* **27** (1988) L2276.
28. M. AVRAMI, *J. Chem. Phys.* **7** (1939) 1103.
29. T. KANAI, T. KAMO and S. P. MATSUDA, *Jpn. J. Appl. Phys.* **28** (1989) L2188.
30. W. ZHU and P. S. NICHOLSON, *J. Mater. Res.* **7** (1992) 38.
31. J. S. LUO, N. M. MERCHANT, E. ESCORCIA-APARICIO, V. A. MARONI, D. M. GRUEN, B. S. TANI, G. N. RILEY and W. L. CARTER, *IEEE Trans. Appl. Supercond.* **3** (1993) 972.
32. J. S. LUO, N. M. MERCHANT, V. A. MARONI, D. M. GRUEN, B. S. TANI, W. L. CARTER and G. N. RILEY, *Appl. Supercond.* **1** (1993) 101.
33. Y. D. CHIU, C. H. KAO, T. S. LEI and M. K. WU, *Physica C* **235–240** (1994) 485.
34. C. H. KAO, Y. D. CHIU, S. L. DUNG, L. C. LEE and M. K. WU, *Mater. Lett* **20** (1994) 83.
35. J.-C. GRIVEL and R. FLÜKIGER, *J. Alloys Comp.* **235** (1996) 53.
36. *Idem., ibid.* **241** (1996) 127.
37. X. P. CHEN, Z. HAN, M. Y. LI, J. MENG and Q. LIU, *Physica C* **391** (2003) 363.
38. R. RAMESH, K. REMSCHNIG, J. M. TARASCON and S. M. GREEN, *J. Mater. Res.* **6** (1991) 278.
39. J. W. ANDERSON, J. A. PARRELL, P. V. P. S. S. SASTRY and D. C. LARBALESTIER, *IEEE Trans. Appl. Supercond.* **7** (1997) 1422.
40. N. MERCHANT, J. S. LUO, V. A. MARONI, G. N. RILEY and W. L. CARTER, *Appl. Phys. Lett.* **65** (1994) 1039.
41. C. B. MAO, L. ZHOU, X. Z. WU and X. Y. SUN, *J. Mater. Sci. Lett.* **17** (1998) 1341.
42. A. K. GALWAY, *Thermochim. Acta* **413** (2004) 139.
43. C. N. R. RAO and K. J. RAO, "Phase Transitions in Solids" (McGraw-Hill, 1978).

Received 15 December 2004
and accepted 14 March 2005